

# Hybridization of G-Quadruplex-Forming Peptide Nucleic Acids to Guanine-Rich DNA Templates Inhibits DNA Polymerase $\eta$ Extension

Connor T. Murphy,<sup>†,§</sup> Anisha Gupta,<sup>‡</sup> Bruce A. Armitage,<sup>§,‡</sup> and Patricia L. Opresko<sup>\*,†,§</sup>

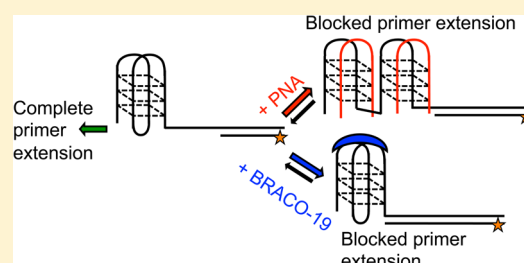
<sup>†</sup>Department of Environmental and Occupational Health, University of Pittsburgh Graduate School of Public Health, Pittsburgh, Pennsylvania 15219, United States

<sup>‡</sup>Department of Chemistry, Carnegie Mellon University, Pittsburgh, Pennsylvania 15213, United States

<sup>§</sup>Center for Nucleic Acids Science and Technology, Carnegie Mellon University, 4400 Fifth Avenue, Pittsburgh, Pennsylvania 15213, United States

## S Supporting Information

**ABSTRACT:** The guanine quadruplex (G-quadruplex) is a highly stable secondary structure that forms in G-rich repeats of DNA, which can interfere with DNA processes, including DNA replication and transcription. We showed previously that short guanine-rich peptide nucleic acids (PNAs) can form highly stable hybrid quadruplexes with DNA. We hypothesized that such structures would provide a stronger block to polymerase extension on G-rich templates than a native DNA homoquadruplex because of the greater thermodynamic stability of the PNA–DNA hybrid structures. To test this, we analyzed the DNA primer extension activity of polymerase  $\eta$ , a translesion polymerase implicated in synthesis past G-quadruplex blocks, on DNA templates containing guanine repeats. We observed a PNA concentration-dependent decrease in the level of polymerase  $\eta$  extension to the end of the template and an increase in the level of polymerase  $\eta$  inhibition at the sequence prior to the G-rich repeats. In contrast, the addition of a complementary C-rich PNA that hybridizes to the G-rich repeats by Watson–Crick base pairing led to a decrease in the level of polymerase inhibition and an increase in the level of full-length extension products. The G-quadruplex-forming PNA exhibited inhibition ( $IC_{50} = 16.2 \pm 3.3$  nM) of polymerase  $\eta$  DNA synthesis on the G-rich templates stronger than that of the established G-quadruplex-stabilizing ligand BRACO-19 ( $IC_{50} = 42.5 \pm 4.8$  nM). Our results indicate that homologous PNA targeting of G-rich sequences creates stable PNA–DNA heteroquadruplexes that inhibit polymerase  $\eta$  extension more effectively than a DNA homoquadruplex. The implications of these results for the potential development of homologous PNAs as therapeutics for halting proliferating cancer cells are discussed.



Guanine quadruplexes (G-quadruplexes) are stable four-stranded secondary structures that form in DNA and RNA sequences containing guanine-rich repeats.<sup>1–4</sup> Their formation has been proposed to be important for gene regulation *in vivo*.<sup>5</sup> Sequences considered likely to form G-quadruplexes that have been identified using computational methods occur at high frequencies near transcription start sites,<sup>6</sup> at the ends of chromosomes in telomeres,<sup>7–9</sup> and in regulatory sequences associated with oncogenes.<sup>10–13</sup> Previous work has focused on targeting G-quadruplex-forming sequences in promoter regions for inhibiting the transcription of oncogenes.<sup>14,15</sup> One example is the c-MYC gene, which encodes a transcription factor that promotes growth and cell cycle progression and is upregulated in many cancer types.<sup>16,17</sup> The NHE-III<sub>1</sub> (nuclease hypersensitivity element III<sub>1</sub>) sequence found in the promoter region of the c-MYC oncogene is guanine-rich and has been shown to form a G-quadruplex *in vitro*.<sup>18</sup> G-Quadruplex binding ligands are being pursued to target and stabilize the G-quadruplex that forms in the c-MYC promoter region to reduce the level of expression of

c-MYC, a growth and cell cycle progression gene that is commonly overexpressed in many cancers.<sup>19–21</sup>

DNA replication begins with the formation of a bubble at an origin of replication. Two replication forks then move in opposite directions away from this bubble as DNA replication progresses.<sup>22</sup> G-Quadruplex barriers to DNA replication fork progression have been implicated in causing breaks and deletions during replication, particularly at common fragile sites and telomeres.<sup>23</sup> Evidence indicates that certain guanine-rich repeats of DNA are particularly active areas for genomic changes, acting as hot spots for nuclease hypersensitivity and rearrangement events.<sup>23–26</sup> More recently, work has shown polymerase  $\eta$  can synthesize through common fragile sequences that are believed to form in noncanonical structures such as hairpins, inverted repeats, and slipped strand misalignments.<sup>27</sup> The ability of translesion synthesis (TLS) polymerases to bypass DNA lesions and adducts is well-established;<sup>28</sup> however,

Received: June 3, 2014

Revised: July 21, 2014

Published: July 28, 2014



the ability of translesion polymerases to bypass these alternative secondary structures in DNA is not well-understood. Previous work suggests the TLS replication machinery may be capable of bypassing G-quadruplex blocks to promote replication fork progression.<sup>29,30</sup> For example, cells deficient in TLS polymerases  $\kappa$  and  $\eta$  are hypersensitive to the G-quadruplex-targeting ligand telomestatin.<sup>29</sup>

G-Quadruplex-targeting ligands are molecules that stabilize preformed G-quadruplexes through either planar stacking<sup>31</sup> or groove binding interactions.<sup>31,32</sup> Such ligands are being pursued in therapeutic strategies that target and stabilize G-quadruplexes in promoter regions, leading to inhibition of target gene expression.<sup>33</sup> There has been some limited success with this approach in gene therapy clinical trials.<sup>34</sup> While these molecules show promise, off-target binding remains a great concern.<sup>35</sup> A second G-quadruplex-targeting therapeutic strategy is to stabilize G-quadruplexes at telomeres.<sup>8,35</sup> Evidence indicates such ligands inhibit binding of the essential shelterin protein complex that caps telomeres and the activity of telomerase, thus leading to rapid shortening of the telomeres in highly proliferative cells such as cancerous cells.<sup>36,37</sup> When telomeres are exhausted, the cells undergo senescence or apoptosis and can no longer divide.<sup>36</sup> Thus, telomeres are an attractive target for halting proliferating cancer cells.

Peptide nucleic acid (PNA) is a synthetic DNA analogue that demonstrates high-affinity binding to DNA in part because of its uncharged backbone.<sup>38,39</sup> PNA molecules that are rich in successive guanines have been shown through biophysical methods to form heteroquadruplexes with DNA and RNA oligonucleotides that are also guanine-rich. This process occurs because of the Hoogsteen base pairing between guanines contributed by the PNA and DNA or RNA and is bolstered by the lack of negative charge on the PNA backbone.<sup>40–44</sup> These intermolecular structures are highly stable, their measured melting temperatures being higher than those of the corresponding intramolecular DNA or RNA G-quadruplexes.<sup>40,41,44</sup>

Previous work demonstrated that various DNA polymerases arrest at G-rich sequences in a manner dependent on the formation and stability of G-quadruplex folding.<sup>45–47</sup> We now report the effects of short G-rich homologous and C-rich complementary PNA oligomers on TLS polymerase  $\eta$  progression on templates with G-quadruplex-forming sequences by using a polymerase extension assay. The sequences used were the NHE-III<sub>1</sub> region of the c-MYC promoter and human telomeric repeats. We provide evidence that a PNA–DNA heteroquadruplex induces a barrier to DNA synthesis greater than that induced by an intramolecular DNA homoquadruplex.

## MATERIALS AND METHODS

**Enzymes and Oligonucleotides.** Recombinant human polymerase  $\eta$  was obtained from Enzymax, flash-frozen in 2.1  $\mu$ L aliquots, and stored at  $-80^{\circ}\text{C}$ . The concentration of the active protein was determined for each lot by quantitating polymerase extension on the G-quadruplex-forming template Myc48 as a standard to control for any preparation to preparation variability. DNA oligonucleotides were obtained from Integrated DNA Technologies, resuspended in 10 mM Tris-HCl (pH 8.0), and stored at  $-20^{\circ}\text{C}$ . Oligonucleotide primers were 5' end labeled with [ $\gamma$ -<sup>32</sup>P]ATP (PerkinElmer) by being incubated for 1 h with optikinase (Affymetrix) at  $37^{\circ}\text{C}$  and purified with a G-25 Sephadex spin column (Amersham Biosciences). Substrates were annealed by mixing a 1:1 ratio of

primer and template oligonucleotides in 10 mM KCl. At this concentration, both full-length and prematurely terminated products were evident in the gel, with the latter corresponding to arrest at the site of the G-quadruplex in the DNA template. At higher KCl concentrations, no full-length product was observed, making it difficult to detect any inhibitory effect of the PNA. Substrates were then heated to  $95^{\circ}\text{C}$  for 5 min and allowed to cool to room temperature overnight. Annealed substrates were stored at  $4^{\circ}\text{C}$ . For PNA addition experiments, the PNA, primer, and template were annealed as described above in 10 mM KCl or 10 mM LiCl. Annealing reactions were conducted at 200 nM DNA template and various concentrations of PNA as indicated in the figure legends.

**Peptide Nucleic Acid Oligomers.** Synthesis of the homologous and complementary PNAs has been described previously.<sup>40,48</sup> *T*-Boc-protected monomers were purchased from Applied Biosystems (discontinued; there are now other commercial vendors for PNA monomers). Peptide nucleic acid (PNA) oligomers were synthesized using standard solid phase synthesis techniques<sup>49,50</sup> and purified by reverse phase high-performance liquid chromatography (HPLC, Waters), and their identities were confirmed by matrix-assisted laser desorption/ionization time-of-flight (MALDI-TOF) mass spectrometry (Applied Biosystems, Voyager DE sSTR) using sinapinic acid as the matrix.

**Polymerase Extension Reactions.** Polymerase  $\eta$  extension reactions were conducted at  $37^{\circ}\text{C}$  in polymerase reaction buffer [0.2% (w/v) BSA, 1 mM DTT, 10 mM Mg(CH<sub>3</sub>COO)<sub>2</sub>, 10 mM KCl, 20 mM Tris-HCl (pH 8), and 250  $\mu$ M dNTP]; 6.7 nM annealed DNA substrate per 10  $\mu$ L reaction mixture was added. Polymerase  $\eta$  was added at an approximate 1:1 enzyme:substrate ratio (normalized by the polymerase activity standard described above) and allowed to extend the primer for 30 min before the reaction was quenched via the addition of 10  $\mu$ L of stop buffer [95% (v/v) formamide, 5 mM EDTA, 0.02% (w/v) xylene cyanol, and 0.02% (w/v) bromophenol blue]. The samples were boiled for 10 min to denature the DNA and then placed on ice immediately before being loaded onto a 10% denaturing polyacrylamide gel. The gels were run at a constant 38 W for 1 h before being exposed to a phosphorimager screen and imaging (Typhoon 9400 Variable Mode Imager).

**Data Processing.** Gel images were processed using ImageQuant version 5.1. Relative synthesis product amounts were determined by dividing the amount of radioactivity in bands for a given product length or lengths by the total radioactivity in the lane. Values were corrected for background in the no enzyme control lane. Graphs were generated using Origin (<http://www.originlab.com>). IC<sub>50</sub> values were calculated using Microsoft Excel. First, the full-length product values at 0 nM PNA or BRACO-19 were set as 0% inhibition. Next, the full-length product values at 33 nM PNA or BRACO-19 were set as 100% inhibition. The percent inhibition was calculated and plotted versus PNA or BRACO-19 concentration and then fit to a linear regression; 50% inhibition according to the linear curve was considered the IC<sub>50</sub> value. The percent of products that were prematurely terminated at positions 1–7 within the six-nucleotide running start (RS) or at the first guanine of the G-rich repeats was quantitated and calculated as a function of total DNA. Calculations of IC<sub>50</sub> values based on prematurely terminated products yielded IC<sub>50</sub> values similar to those based on full-length products (data not shown).

# RESULTS

Previous work indicates that DNA secondary structures may act as impediments to DNA synthesis by DNA polymerases during S phase.<sup>23</sup> Polymerase extension assays have been used successfully to analyze the effectiveness of G-quadruplex-stabilizing ligands.<sup>51</sup> Therefore, to investigate the potential effectiveness of PNA–DNA heteroquadruplexes to interfere with DNA processing and metabolism, we analyzed polymerase  $\eta$  synthesis activity on model G-quadruplex-forming sequences derived from biologically relevant sequences in the genome (Figure 1). For this, we designed oligonucleotides containing

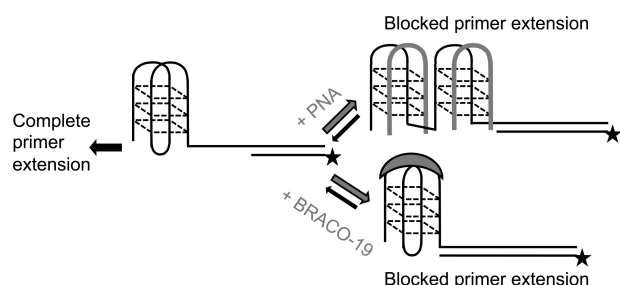


**Figure 1.** Model of polymerase extension inhibition by formation of stable PNA–DNA G-quadruplex structural blocks. More stable complexes formed by peptide nucleic acid oligomers (gray lines) or G-quadruplex binding ligands are expected to shift the equilibrium to a higher-stability structure, leading to a greater inhibition of synthesis.

either the NHE-III<sub>1</sub> region of the *c-MYC* oncogene promoter (**Myc48**) or four tandem human telomeric repeats, (TTAGGG)<sub>4</sub> (**hTelo54**) (Table 1), and examined polymerase activity in the presence of the homologous guanine-rich 8-mer PNA **P<sub>myc-H</sub>** or the complementary cytosine-rich 8-mer PNA **P<sub>myc-C</sub>**. These DNA sequences were chosen because of their biological relevance and their previously established ability to form a complex with the homologous **P<sub>myc-H</sub>** PNA.<sup>40</sup> A KCl concentration of 10 mM was used instead of a physiological KCl concentration of 100–150 mM because of undetectable synthesis product past the apparent block at the start of the G-quadruplex-forming sequence by the polymerase at a KCl concentration of 100 mM even in the absence of PNA (data not shown).

## The Level of Polymerase $\eta$ Progression Is Reduced on G-Rich Templates as a Function of PNA Concentration.

**P<sub>myc-H</sub>** contains two G-tracts with an intervening loop sequence and was designed to be perfectly homologous to the NHE-III<sub>1</sub> sequence of the *c-Myc* promoter. This PNA sequence, however, is expected to bind to any guanine quadruplex-forming sequence because the Hoogsteen base pairing with

DNA requires only the presence of guanines in the PNA; the loop does not participate in binding. Therefore, one PNA may be used for targeting multiple sequences. This PNA has been confirmed to bind to both the *c-Myc* G-quadruplex and the human telomere repeat with low nanomolar  $K_D$  values.<sup>52</sup> For the research described here, model G-quadruplex-forming oligonucleotides **Myc48** and **hTelo54** and control oligonucleotide **NoGQ48** were annealed to radiolabeled primer **RS6** in 10 mM KCl. Annealing reaction mixtures contained increasing concentrations of **P<sub>myc-H</sub>** PNA (from 0 to 5000 nM). The annealed substrates were subsequently added to reaction mixtures for polymerase  $\eta$  extension. The primer design allowed a six-nucleotide running start before the guanine repeats. For the **Myc48** and **hTelo54** templates, we observed a notable site of inhibition at the end of the running start (indicated by the dotted arrow) where the polymerase encounters the first guanine repeat (Figure 2A,B and Figure S1 of the Supporting Information). This site of inhibition is not apparent in the **NoGQ48** control that lacks G-quadruplex-forming sequences (Figure 2C). For the **Myc48** and **hTelo54** templates, we also observed a decrease in the level of synthesis to the end of the template (Figure 2A,B, indicated by the top arrow) as a function of homologous PNA concentration, and a corresponding increase in the amount of products terminated prior to the guanine repeats within the RS (see Figure S2 of the Supporting Information for quantitation). The full-length product was not detected or was reduced 3-fold for the **Myc48** or **hTelo54** template, respectively, at 33 nM PNA. Interestingly, the major arrest site shifts closer to the proximal end of the quadruplex-forming sequence in the presence of the PNA. We ascribe this result to the thermodynamically more stable PNA–DNA heteroquadruplex, which should be more difficult for the polymerase enzyme to invade to extend the primer at least partially into the quadruplex region. No significant reduction in the level of polymerase progression was observed for the **NoGQ48** template at 33 nM PNA, but a 2-fold decrease was apparent at 167 nM, suggesting that, at the highest concentration, the PNA exerts some nonspecific effects. Therefore, all comparisons are made to 33 nM PNA. The calculated  $IC_{50}$  value for **P<sub>myc-H</sub>** PNA inhibition of complete DNA synthesis (full-length product) is  $16.2 \pm 3.3$  nM for the **Myc48** template and  $25.4 \pm 3.8$  nM for the **hTelo54** template.

Thermal stability is dependent on the ionic content of the solution, with potassium having a stabilizing effect greater than that of lithium for both intramolecular<sup>53</sup> and intermolecular G-quadruplexes.<sup>44</sup> When **P<sub>myc-H</sub>** was annealed to the **Myc48** template in reaction mixtures containing 10 mM LiCl, the level of progression of the polymerase on this substrate was dramatically increased. This indicates that the **P<sub>myc-H</sub>** blockage

**Table 1.** Sequences and Oligonucleotides Used<sup>a</sup>

DNA name	sequence (5'–3')
<b>Myc48</b>	AGG GTG GGG AGG GTG GGG TCT CGC GGC CAT AGC AAC CGA CGT ACG GCG
<b>hTelo54</b>	TTA <u>GGG TTA GGG</u> TTA <u>GGG TTA GGG</u> TCT CGC GGC CAT AGC AAC CGA CGT ACG GCG
<b>MycComp</b>	CCC <u>CAC CCT CCC CAC</u> CCT TCT CGC GGC CAT AGC AAC CGA CGT ACG GCG
<b>NoGQ48</b>	AAT CCA CCG TTG AGC CCA TCT CGC GGC CAT AGC AAC CGA CGT ACG GCG
primer <b>RS6</b>	CGC CGT ACG TCG GTT GCT ATG GCC
PNA name	sequence (N–C)
<b>P<sub>myc-H</sub></b>	H-GGGAGGGG-Lys-NH <sub>2</sub>
<b>P<sub>myc-C</sub></b>	H-CCCCCCCC-Lys-NH <sub>2</sub>

<sup>a</sup>Predicted PNA binding sites are underlined.



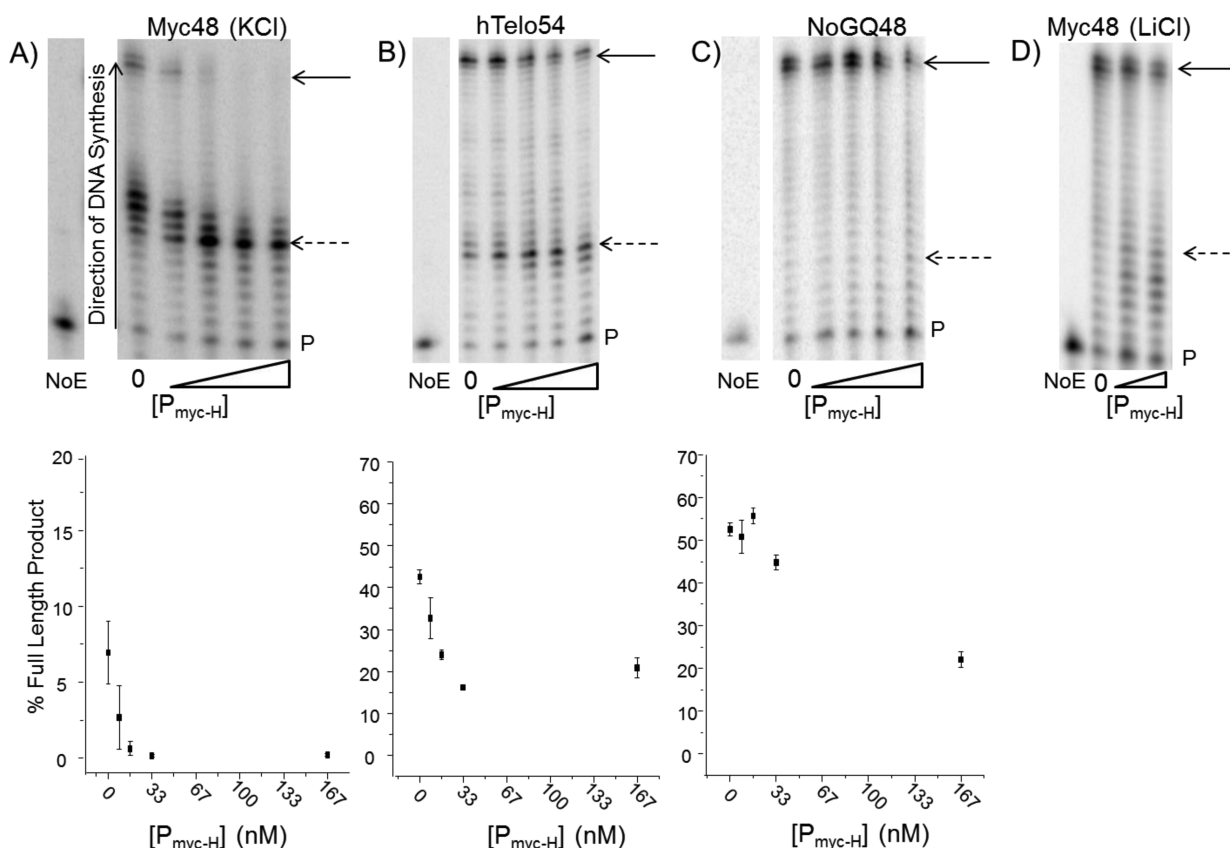


**Figure 2.** PNA concentration-dependent inhibition of polymerase  $\eta$  progression on guanine-rich templates. Template DNAs **Myc48** (A and D), **hTelo54** (B), and **NoGQ48** (C) were annealed to a radiolabeled primer that provided a six-nucleotide running start prior to the guanine repeat region of the template and the PNA oligomer  $P_{\text{myc-H}}$  binding site. Annealing reaction mixtures contained 200 nM DNA and either 0, 250, 500, 1000, or 5000 nM PNA in 10 mM KCl (A–C) or 0, 500, or 1000 nM PNA in 10 mM LiCl (D). Substrates were diluted 1:30 into the polymerase reaction mixtures, which contained final concentrations of 6.7 nM DNA and 0–167 nM PNA (A–C) or 0, 16.7, or 33.3 nM PNA (D). Reactions were initiated via the addition of 6.7 nM polymerase  $\eta$  (normalized by activity), and mixtures were incubated for 30 min before reactions were quenched. Reaction products were analyzed on a 10% polyacrylamide denaturing gel. Top arrows indicate the full-length product. Dotted arrows correspond to the end of the running start. P marks the primer band. Full-length products were quantitated. The percent of primers extended to the final base was calculated as the ratio of total radioactivity in the lane. Data are means and standard deviations of three experiments.

observed in KCl is ion-dependent and requires  $P_{\text{myc-H}}$  G-quadruplex formation with the template (Figure 2D). This difference is not due to salt effects on the enzyme as there is little difference in synthesis in solutions containing KCl or LiCl on the **NoGQ48** control substrate (Figure 1C and Figure S3 of the Supporting Information, respectively).

**Influence of Complementary PNA Binding on Polymerase  $\eta$  Progression.** PNA oligomers are traditionally designed to bind by complementary canonical Watson–Crick base pairing to DNA or RNA target sequences of biological relevance for sequence detection (e.g., *in situ* hybridization)<sup>54,55</sup> or gene targeting.<sup>56</sup> This contrasts to the G-quadruplex PNA homologous binding, which involves G-tetrad formation, stabilized by guanine–guanine Hoogsteen base pairing. Therefore, we wished to compare the effects on polymerase extension of complementary PNA binding to form a PNA–DNA heteroduplex to the effects we observed with the PNA–DNA heteroquadruplexes. We analyzed polymerase  $\eta$  synthesis on guanine-rich DNA template **Myc48** after targeting with cytosine-rich PNA oligomer  $P_{\text{myc-C}}$ . In this case, we observed a moderate (2.6-fold) increase in the level of synthesis to the end of the template sequence, as well as a shift in the location of the polymerase inhibition sites to the expected two  $P_{\text{myc-C}}$  PNA binding sites on the **Myc48** template (Figure 3A).

Conversely, we annealed guanine-rich 8-mer PNA  $P_{\text{myc-H}}$  to cytosine-rich DNA sequence **MycComp**, which is the sequence complementary to **Myc48**. We observed a minor (1.2-fold) decrease in the amount of full-length product at a high PNA concentration (33 nM) accompanied by a small accumulation of prematurely terminated products at the predicted PNA binding site (Figure 3A, dotted arrow; see Figure S4 of the Supporting Information for quantitation of products terminated prior to G-rich repeats). Quantitation of the products terminated at positions 1–7 at the first predicted PNA binding site (RS) or positions 8–23 at the second predicted PNA binding sites (marked by dotted arrows) is shown in panels A and B of Figure S4 of the Supporting Information. The Watson–Crick binding by the PNA weakly inhibits synthesis on unstructured templates, whereas Watson–Crick binding by PNA stimulates synthesis on the G-quadruplex-forming template. This suggests the 8-mer PNA–DNA Watson–Crick base pairing fails to form a duplex sufficiently stable to inhibit the polymerase extension. At 167 nM PNA, we observe two strong inhibition sites and an increase in the total level of synthesis through the **Myc48** template, despite the predicted nonspecific effects of the PNA. The level of full-length synthesis along the **MycComp** sequence is decreased at 167 nM PNA, and a weak inhibition site is observed at the predicted binding

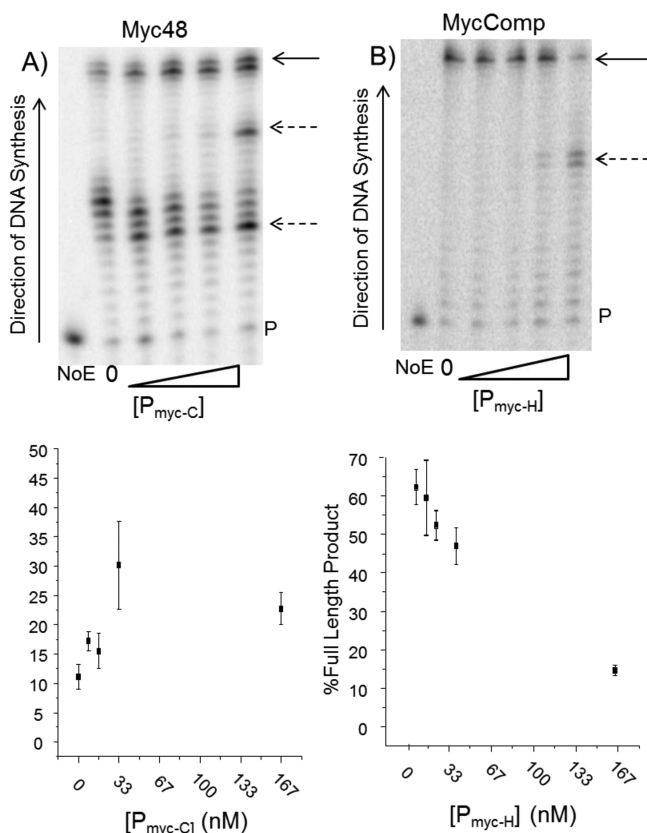


**Figure 3.** Modulation of polymerase  $\eta$  extension by complementary PNA binding. Template DNAs **Myc48** (A) and **MycComp** (B) (200 nM) were annealed to a primer that provided a six-nucleotide running start prior to the guanine repeat region of the template and increasing concentrations (from 0 to 5000 nM) of either complementary PNA **P<sub>myc-C</sub>** (A) or **P<sub>myc-H</sub>** (B). Annealed substrates were diluted 1:30 into the polymerase reaction mixtures, which contained final concentrations of 6.7 nM DNA substrate and 0–167 nM PNA. Reactions were initiated via the addition of 6.7 nM polymerase  $\eta$  (normalized by activity), and mixtures were incubated for 30 min before reactions were quenched. Reaction products were analyzed on a 10% polyacrylamide denaturing gel. Top arrows indicate the full-length product. Dotted arrows indicate the predicted binding site(s) of the PNA. P marks the primer band. The full-length product was quantitated. The percent of primers extended to the final base was calculated as a ratio of total radioactivity in the lane. Data are means and standard deviations of three experiments.

site; however, these effects may be nonspecific because of our observations in Figure 2.

**BRACO-19 Inhibits Polymerase  $\eta$  Extension on the G-Rich Myc48 Template.** Next we compared the polymerase inhibition we observed with the G-quadruplex-forming PNA to that observed with a well-established DNA G-quadruplex-stabilizing ligand, BRACO-19.<sup>57–59</sup> For this, we measured polymerase extension on the guanine-rich **Myc48** template in the presence of BRACO-19 at concentrations identical to the PNA concentrations tested. First, the **Myc48** template was annealed to the primer in the presence of increasing BRACO-19 concentrations (from 0 to 5000 nM) using the same annealing reaction conditions that were used for the homologous and complementary PNA experiments. As seen for the PNA, we observed a BRACO-19-dependent decrease in the amount of full-length polymerase product and an increase in the amount of short products terminated at the site

corresponding to the start of the guanine repeats ( $IC_{50} = 42.5 \pm 4.8$  nM) (Figure 4A and Figure S5A of the Supporting

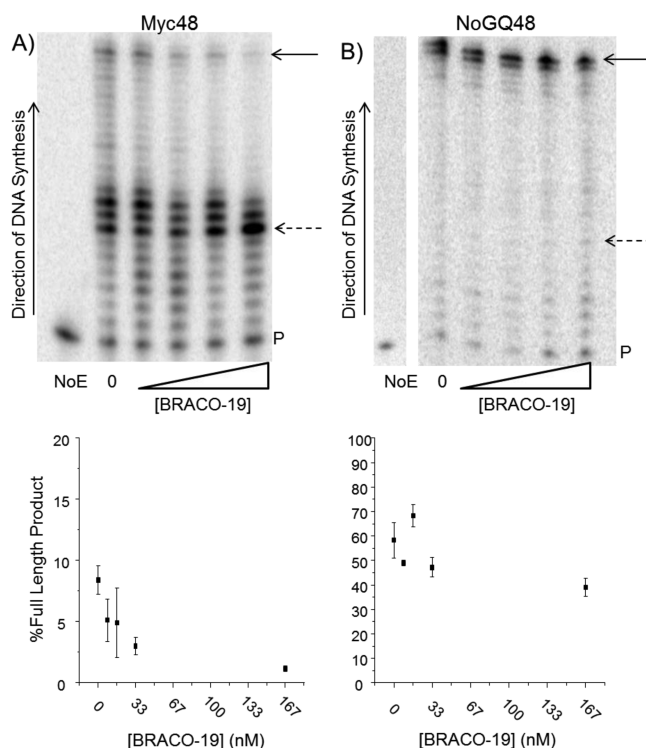


**Figure 4.** BRACO-19 concentration-dependent inhibition of polymerase  $\eta$  extension on guanine-rich DNA templates. Template DNA **Myc48** (200 nM) was annealed to a primer that provided a six-nucleotide running start prior to the guanine repeat region of the template, in the presence of increasing concentrations of the G-quadruplex-stabilizing ligand BRACO-19 (from 0 to 5000 nM). Annealed substrates were diluted 1:30 into the polymerase reaction mixtures containing final concentrations of 6.7 nM DNA substrate and 0–167 nM BRACO-19. Reactions were initiated via the addition of 6.7 nM polymerase  $\eta$  and conducted for 30 min before being quenched. Reaction products were analyzed on a 10% polyacrylamide denaturing gel. Top arrows indicate the full-length product. Bottom arrows indicate the end of the running start. P marks the primer band. The full-length product was quantitated. The percent of primers extended to the final base was calculated as a ratio of total radioactivity in the lane. Data are means and standard deviations of three experiments.

Information). In contrast, no significant polymerase inhibition was observed on **NoGQ48** templates that were prepared in annealing reaction mixtures containing increasing concentrations of BRACO-19 (Figure 4B and Figure S5B of the Supporting Information). This indicates that BRACO-19 does not nonspecifically inhibit the enzyme at the compound concentrations tested.

## DISCUSSION

Previous biophysical studies have demonstrated the ability of guanine-rich PNA to form stable heteroquadruplexes with homologous DNA targets.<sup>40,44</sup> Here we demonstrate that such heteroquadruplex structures inhibit DNA polymerase extension. We have compared the inhibition of human polymerase  $\eta$  by homologous quadruplex-forming PNA (Figure 2 and Figure S2 of the Supporting Information) to that of complementary duplex-forming PNA (Figure 3), as well as that of a G-quadruplex-stabilizing ligand BRACO-19 (Figure 4).

While the native DNA G-quadruplex inhibits polymerase progression on the **Myc48** and **hTelo54** templates, some DNA synthesis through the sequence is observed (Figure 2A,B, 0 nM PNA). This inhibition is greatly accelerated when the G-rich  $P_{\text{myc-H}}$  PNA molecule is introduced. The  $P_{\text{myc-H}}$  PNA concentration-dependent inhibition of full-length DNA synthesis on guanine-rich templates, and concurrent increase in prematurely terminated products at the predicted heteroquadruplex site, strongly suggests that PNA G-quadruplex formation with the DNA template hinders the advancement of the polymerase (Figure 2 and Figure S2 of the Supporting Information). Consistent with this, suppression of PNA G-quadruplex formation with the DNA by annealing the substrates in LiCl relieved the polymerase inhibition (Figure 2D). To the best of our knowledge, this represents the first evidence that a PNA–DNA heteroquadruplex can inhibit DNA synthesis. The effective concentration levels are comparable to those of the previously tested BRACO-19 G-quadruplex ligand (Figures 2 and 4). The  $IC_{50}$  values are both in the midnanomolar range (10–50 nM). The  $IC_{50}$  for the PNA is higher than the  $K_D$  of 5 nM determined previously by surface plasmon resonance experiments.<sup>40</sup> The differences may be related to how the polymerase engages and processes the substrate or more likely the KCl concentration that is lower than that used in the SPR experiments, which would lead to lower heteroquadruplex stability.

Strand displacement DNA synthesis is a process by which an advancing polymerase can displace a downstream DNA strand that is base paired to the template strand. This process occurs at Okazaki fragments.<sup>60</sup> While polymerase  $\eta$  has been shown to engage in strand displacement synthesis,<sup>61</sup> the higher affinity of the PNA for the target DNA may account for the reduction in the level of strand displacement when the PNA is involved. It is important to note that the polymerase assay does not directly measure binding, but rather read-through of the polymerase. If strand displacement DNA synthesis is occurring in the case of the PNA, it may influence the  $IC_{50}$  value. Interestingly, the  $K_D$  values for binding of  $P_{\text{myc-H}}$  to **Myc48** and **hTelo54** at 100 mM KCl are different by a factor of 2.5, although these values were determined at a KCl concentration (100 mM) higher than that used in the experiments (10 mM in our experiments). The  $IC_{50}$  values also differ by a factor of 2.5. The telomeric G-quadruplex was targeted somewhat less effectively by the homologous PNA, compared to the **Myc48** template (Figure 2), as indicated by a higher  $IC_{50}$ . This may be due to the slightly lower affinity of the PNA for the telomeric G-quadruplex using the 100 mM KCl values as a guide to binding stability.

The complementary PNA binding and PNA–DNA heteroduplex results are complex (Figure 3 and Figure S4 of the Supporting Information). Previous work has shown that there are kinetic and thermodynamic considerations that affect the binding of complementary PNAs to target G-quadruplexes.<sup>48</sup> Specifically, a higher stability of the native G-quadruplex will lead to slower binding kinetics of complementary PNAs. This stability can be affected by ionic content or structural factors of the native G-quadruplex. In this work, the addition of PNA can either stimulate synthesis (A) or slightly inhibit synthesis (B) depending on the target sequence. There is a low level of inhibition by complementary binding of guanine-rich  $P_{\text{myc-H}}$  to cytosine-rich template **MycComp**. There is apparent stimulation of polymerase  $\eta$  extension when a C-rich PNA complementarily binds G-quadruplex-forming template **Myc48**. This is likely due to the binding of the PNA to the

DNA strand forming a PNA–DNA duplex, which prevents that DNA strand from folding into an intramolecular G-quadruplex. This suggests that an intramolecular DNA G-quadruplex presents a stronger block to the polymerase than a short PNA–DNA heteroduplex. However, at the higher  $P_{\text{myc-C}}$  PNA concentrations, prematurely terminated products are observed at the two predicted PNA binding sites (Figure 3A, dotted arrows), which support the conclusion that the PNA was bound to the template but could be partly disrupted by the advancing polymerase. Tellam and colleagues recently reported on targeting a complementary oligonucleotide to a G-quadruplex-forming mRNA motif. When the complementary oligonucleotide was bound, they observed an apparent increase in the level of read-through of the sequence and a corresponding increase in the level of translation of the message.<sup>62</sup>

Although prior work demonstrated 14-fold faster hybridization of  $P_{\text{myc}}$  to Myc- versus hTelo-derived quadruplexes, the affinities differed by a factor of only 2.5.<sup>52</sup> The results presented here also demonstrate that  $P_{\text{myc}}$  is capable of binding to both quadruplexes, because polymerase progression was blocked on templates **Myc48** and **hTelo54**. Thus, the selectivity in targeting different G-quadruplexes is relatively low, at least in cases in which equilibrium is reached. While selectivity need not be high in cases in which global inhibition of gene expression is desirable (e.g., anticancer or antibiotic strategies, provided delivery to targeted cells is selective), the large number of quadruplex-forming sequences in genomic DNA and RNA likely precludes selective targeting of single DNA or RNA quadruplexes within a cell. Extending the recognition beyond the quadruplex-forming sequence to include flanking bases is one strategy for enhancing selectivity and is currently under investigation.

The results in total provide evidence supporting the inhibition of DNA polymerase synthesis at G-quadruplex-forming sequences by employing short homologous G-rich PNAs. Guanine quadruplexes have already garnered interest as transcriptional regulators<sup>14</sup> as well as elements that can interfere with telomere replication.<sup>37</sup> Common cancer therapies target DNA replication and include cross-linking agents such as cisplatin.<sup>9</sup> The inhibition of DNA polymerase at G-quadruplex-forming sites provides an alternative strategy for inhibiting DNA synthesis at selective regions in the genome. For example, G-quadruplex ligands were shown to inhibit telomeric DNA synthesis and cause telomere shortening.<sup>37</sup> Our results show that G-quadruplex-stabilizing ligand BRACO-19 inhibits polymerase  $\eta$  read-through of a quadruplex-forming sequence with an  $IC_{50}$  that is higher than, but in the same midnanomolar range as, that of  $P_{\text{myc-H}}$ . Future development of quadruplex-forming PNAs for improved biochemical and biological activity will focus on backbone variations to optimize specificity<sup>63</sup> and allow cell uptake.<sup>64</sup>

## ■ ASSOCIATED CONTENT

### ● Supporting Information

Figures that demonstrate the inhibitory effect of the PNA at concentrations lower than those described in the text and an alternative quantitation of the synthesis and inhibition by measurement of the amount of products stalled before the predicted G-quadruplex-forming region. This material is available free of charge via the Internet at <http://pubs.acs.org>.



## AUTHOR INFORMATION

### Corresponding Author

\*Bridgeside Point, 100 Technology Dr., Suite 326, Pittsburgh, PA 15219. E-mail: plo4@pitt.edu. Phone: (412) 624-8285. Fax: (412) 624-9361.

### Funding

This work was supported by the DSF Charitable Foundation through the Center for Nucleic Acids Science and Technology (P.L.O. and B.A.A.).

### Notes

The authors declare no competing financial interest.

## ABBREVIATIONS

G-quadruplex, guanine quadruplex; PNA, peptide nucleic acid; NHE-III<sub>1</sub>, nuclease hypersensitivity element III<sub>1</sub>; TLS, translesion synthesis; RS, running start.

## REFERENCES

- (1) Davis, J. T. (2004) G-Quartets 40 Years Later: From 5'-GMP to Molecular Biology and Supramolecular Chemistry. *Angew. Chem., Int. Ed.* 43, 668–698.
- (2) Simonsson, T. (2001) G-Quadruplex DNA Structures: Variations on a Theme. *Biol. Chem.* 382, 621–628.
- (3) Sen, D., and Gilbert, W. (1990) A sodium-potassium switch in the formation of four-stranded G4 DNA. *Nature* 344, 410–414.
- (4) Sen, D., and Gilbert, W. (1988) Formation of parallel four-stranded complexes by guanine-rich motifs in DNA and its implications for meiosis. *Nature* 334, 364–366.
- (5) Cogoi, S., and Xodo, L. E. (2006) G-quadruplex formation within the promoter of the KRAS proto-oncogene and its effect on transcription. *Nucleic Acids Res.* 34, 2536–2549.
- (6) Huppert, J., and Parkinson, G. (2007) G-Quadruplexes in Promoters Throughout the Human Genome. *Nucleic Acids Res.* 35, 406–413.
- (7) Mergny, J.-L., Riou, J.-F., Mailliet, P., Teulade-Fichou, M.-P., and Gilson, E. (2002) Natural and pharmacological regulation of telomerase. *Nucleic Acids Res.* 30, 839–865.
- (8) Neidle, S., and Parkinson, G. (2002) Telomere maintenance as a target for anticancer drug discovery. *Nat. Rev. Drug Discovery* 1, 383–393.
- (9) Hurley, L. H. (2002) DNA and its associated processes as targets for cancer therapy. *Nat. Rev. Cancer* 2, 188–200.
- (10) De Armond, R., Wood, S., Sun, D., Hurley, L. H., and Ebbinghaus, S. W. (2005) Evidence for the Presence of a Guanine Quadruplex Forming Region within a Polypurine Tract of the Hypoxia Inducible Factor 1 $\alpha$  Promoter. *Biochemistry* 44, 16341–16350.
- (11) Dai, J., Dexheimer, T. S., Chen, D., Carver, M., Ambrus, A., Jones, R. A., and Yang, D. (2006) An Intramolecular G-Quadruplex Structure with Mixed Parallel/Antiparallel G-Strands Formed in the Human BCL-2 Promoter Region in Solution. *J. Am. Chem. Soc.* 128, 1096–1098.
- (12) Fernando, H., Reszka, A. P., Huppert, J., Ladame, S., Rankin, S., Venkitaraman, A. R., Neidle, S., and Balasubramanian, S. (2006) A Conserved Quadruplex Motif Located in a Transcription Activation Site of the Human c-kit Oncogene. *Biochemistry* 45, 7854–7860.
- (13) Simonsson, T., and Sjöback, R. (1999) DNA Tetraplex Formation Studied with Fluorescence Resonance Energy Transfer. *J. Biol. Chem.* 274, 17379–17383.
- (14) Siddiqui-Jain, A., Grand, C. L., Bearss, D. J., and Hurley, L. H. (2002) Direct Evidence for a G-Quadruplex in a Promoter Region and its Targeting with a Small Molecule to Repress c-MYC Transcription. *Proc. Natl. Acad. Sci. U.S.A.* 99, 11593–11598.
- (15) Lemarteleur, T., Gomez, D., Paterski, R., Mandine, E., Mailliet, P., and Riou, J.-F. (2004) Stabilization of the c-myc Gene Promoter Quadruplex by Specific Ligands' Inhibitors of Telomerase. *Biochem. Biophys. Res. Commun.* 323, 802–808.

- (16) Dang, C. V. (1999) c-Myc Target Genes Involved in Cell Growth, Apoptosis, and Metabolism. *Mol. Cell. Biol.* 19, 1–11.
- (17) Hermeking, H. (2003) The MYC Oncogene as a Cancer Drug Target. *Curr. Cancer Drug Targets* 3, 163–175.
- (18) Phan, A. T., Modi, Y. S., and Patel, D. J. (2004) Propeller-Type Parallel-Stranded G-Quadruplexes in the Human c-myc Promoter. *J. Am. Chem. Soc.* 126, 8710–8716.
- (19) Balasubramanian, S., Hurley, L. H., and Neidle, S. (2011) Targeting G-quadruplexes in gene promoters: A novel anticancer strategy? *Nat. Rev. Drug Discovery* 10, 261–275.
- (20) Ou, T.-M., Lu, Y.-J., Zhang, C., Huang, Z.-S., Wang, X.-D., Tan, J.-H., Chen, Y., Ma, D.-L., Wong, K.-Y., Tang, J. C.-O., Chan, A. S.-C., and Gu, L.-Q. (2007) Stabilization of G-Quadruplex DNA and Down-Regulation of Oncogene c-myc by Quindoline Derivatives. *J. Med. Chem.* 50, 1465–1474.
- (21) Shalaby, T., Bueren, A. O. v., Hürlimann, M.-L., Fiaschetti, G., Castelletti, D., Masayuki, T., Nagasawa, K., Arcaro, A., Jelesarov, I., Shin-ya, K., and Grotzer, M. (2010) Disabling c-Myc in Childhood Medulloblastoma and Atypical Teratoid/Rhabdoid Tumor Cells by the Potent G-Quadruplex Interactive Agent S2T1-6OTD. *Mol. Cancer Ther.* 9, 167–169.
- (22) Jones, R. M., and Petermann, E. (2012) Replication fork dynamics and the DNA damage response. *Biochem. J.* 443, 13–26.
- (23) Bacolla, A., and Wells, R. D. (2004) Non-B DNA Conformations, Genomic Rearrangements, and Human Disease. *J. Biol. Chem.* 279, 47411–47414.
- (24) Lopes, J., Piazza, A. I., Bermejo, R., Kriegsmann, B., Colosio, A., Teulade-Fichou, M.-P., Foiani, M., and Nicolas, A. (2011) G-quadruplex-induced instability during leading-strand replication. *EMBO J.* 30, 4033–4046.
- (25) Wang, G., and Vasquez, K. M. (2004) Naturally occurring H-DNA-forming sequences are mutagenic in mammalian cells. *Proc. Natl. Acad. Sci. U.S.A.* 101, 13448–13453.
- (26) Wang, G., Carbajal, S., Vijg, J., DiGiovanni, J., and Vasquez, K. M. (2012) DNA Structure-induced Genomic Instability In Vivo. *J. Natl. Cancer Inst.* 100, 1815–1817.
- (27) Bergoglio, V., Boyer, A.-S., Naim, E. W. V., Legube, G., Lee, M. Y. W. T., Rey, L., Rosselli, F., Cazaux, C., Eckert, K. A., and Hoffman, J.-S. (2013) DNA synthesis by Pol  $\eta$  promotes fragile site stability by preventing under-replicated DNA in mitosis. *J. Cell Biol.* 201, 395–408.
- (28) Kusumoto, R., Masutani, C., Iwai, S., and Hanaoka, F. (2002) Translesion Synthesis by Human DNA Polymerase  $\eta$  across Thymine Glycol Lesions. *Biochemistry* 41, 6090–6099.
- (29) Bétous, R., Rey, L., Wang, G., Pillaire, M.-J., Puget, N., Selves, J., Biard, D. S. F., Shin-ya, K., Vasquez, K. M., Cazaux, C., and Hoffmann, J.-S. (2009) Role of TLS DNA polymerases  $\eta$  and  $\kappa$  in processing naturally occurring structured DNA in human cells. *Mol. Carcinog.* 48, 369–378.
- (30) Sarkies, P., Reams, C., Simpson, L. J., and Sale, J. E. (2010) Epigenetic instability due to defective replication of structured DNA. *Mol. Cell* 40, 703–713.
- (31) Neidle, S. (2009) The structures of quadruplex nucleic acids and their drug complexes. *Curr. Opin. Struct. Biol.* 19, 239–250.
- (32) Jain, A. K., and Bhattacharya, S. (2011) Interaction of G-Quadruplexes with Nonintercalating Duplex-DNA Minor Groove Binding Ligands. *Bioconjugate Chem.* 22, 2355–2368.
- (33) Brooks, T. A., and Hurley, L. H. (2010) Targeting MYC Expression through G-Quadruplexes. *Genes Cancer* 1, 641–649.
- (34) Balasubramanian, S., and Neidle, S. (2009) G-quadruplex nucleic acids as therapeutic targets. *Curr. Opin. Chem. Biol.* 13, 345–353.
- (35) Chen, C.-y., Wang, Q., Liu, J.-q., Hao, Y.-h., and Tan, Z. (2011) Contribution of Telomere G-Quadruplex Stabilization to the Inhibition of Telomerase-Mediated Telomere Extension by Chemical Ligands. *J. Am. Chem. Soc.* 133, 15036–15044.
- (36) Palm, W., and Lange, T. d. (2008) How Shelterin Protects Mammalian Telomeres. *Annu. Rev. Genet.* 42, 301–304.

- (37) Rizzo, A., Salvati, E., Porru, M., D'Angelo, C., Stevens, M. F., D'Incalci, M., Leonetti, C., Gilson, E., Zupi, G., and Biroccio, A. (2009) Stabilization of quadruplex DNA perturbs telomere replication leading to the activation of an ATR-dependent ATM signaling pathway. *Nucleic Acids Res.* 37, 5353–5364.
- (38) Ray, A., and Nordén, B. (2000) Peptide Nucleic Acid (PNA): Its Medical and Biotechnical Applications and Promise for the Future. *FASEB J.* 14, 1041–1060.
- (39) Lohse, J., Dahl, O., and Nielsen, P. E. (1999) Double Duplex Invasion by Peptide Nucleic Acid: A General Principle for Sequence-Specific Targeting of Double-Stranded DNA. *Proc. Natl. Acad. Sci. U.S.A.* 96, 11804–11808.
- (40) Roy, S., Tanious, F., Wilson, W. D., Ly, D. H., and Armitage, B. A. (2007) High Affinity Homologous Peptide Nucleic Acid Probes for Targeting a Quadruplex Forming Sequence from a MYC Promoter Element. *Biochemistry* 46, 10433–10443.
- (41) Datta, B., Schmitt, C., and Armitage, B. A. (2003) Formation of a PNA2-DNA2 Hybrid Quadruplex. *J. Am. Chem. Soc.* 125, 4111–4118.
- (42) Datta, B., Bier, M. E., Roy, S., and Armitage, B. A. (2005) Quadruplex Formation by a Guanine-Rich PNA Oligomer. *J. Am. Chem. Soc.* 127, 4199–4207.
- (43) Marin, V. L., and Armitage, B. A. (2005) RNA Guanine Quadruplex Invasion by Complementary and Homologous PNA Probes. *J. Am. Chem. Soc.* 127, 8032–8033.
- (44) Lusvardi, S., Murphy, C. T., Roy, S., Tanious, F. A., Sacui, I., Wilson, W. D., Ly, D. H., and Armitage, B. A. (2009) Loop and Backbone Modifications of Peptide Nucleic Acid Improve G-quadruplex Binding Selectivity. *J. Am. Chem. Soc.* 131, 18145–181424.
- (45) Sun, D., and Hurley, L. H. (2010) Biochemical Techniques for the Characterization of G-Quadruplex Structures: EMSA, DMS Footprinting, and DNA Polymerase Stop Assay. *Methods Mol. Biol.* 608, 65–79.
- (46) Kumari, D., Lokanga, R., Yudkin, D., Zhao, X.-N., and Usdin, K. (2012) Chromatin changes in the development and pathology of the Fragile X-associated disorders and Friedreich ataxia. *Biochim. Biophys. Acta* 1819, 802–810.
- (47) Woodford, K. J., Howell, R. M., and Usdin, K. (1994) A Novel K<sup>+</sup>-dependent DNA Synthesis Arrest Site in a Commonly Occurring Sequence Motif in Eukaryotes. *J. Biol. Chem.* 269, 27029–27035.
- (48) Gupta, A., Lee, L. L., Roy, S., Tanious, F. A., Wilson, W. D., Ly, D. H., and Armitage, B. A. (2013) Strand invasion of DNA quadruplexes by PNA: Comparison of homologous and complementary hybridization. *ChemBioChem* 14, 1476–1484.
- (49) Koch, T. (1999) PNA Oligomer Synthesis by Boc Chemistry. In *Peptide Nucleic Acids* (Nielsen, P. E., and Egholm, M., Eds.) pp 21–37, Horizon Scientific Press, Norfolk, U.K.
- (50) Christensen, L., Fitzpatrick, R., Gildea, B., Petersen, K. H., Hansen, H. F., Koch, T., Egholm, M., Buchardt, O., Nielsen, P. E., Coull, J., and Berg, R. H. (1995) Solid-Phase Synthesis of Peptide Nucleic Acids. *J. Pept. Sci.* 3, 175–183.
- (51) Han, H., Hurley, L. H., and Salazar, M. (1999) A DNA polymerase stop assay for G-quadruplex-interactive compounds. *Nucleic Acids Res.* 27, 537–542.
- (52) Roy, S., Zanotti, K. J., Murphy, C. T., Tanious, F. A., Wilson, W. D., Ly, D. H., and Armitage, B. A. (2011) Kinetic discrimination in recognition of DNA quadruplex targets by guanine-rich heteroquadruplex-forming PNA probes. *Chem. Commun.* 47, 8524–8526.
- (53) Williamson, J. R. (1994) G-Quartet Structures in Telomeric DNA. *Annu. Rev. Biophys. Biomol. Struct.* 23, 703–730.
- (54) Socher, E., Knoll, A., and Seitz, O. (2012) Dual fluorophore PNA FIT-probes: Extremely responsive and bright hybridization probes for the sensitive detection of DNA and RNA. *Org. Biomol. Chem.* 10, 7363–7371.
- (55) Blanco, A. M., and Artero, R. (2010) A practical approach to FRET-based PNA fluorescence *in situ* hybridization. *Methods* 52, 343–351.
- (56) Thomas, S. M., Sahu, B., Rapireddy, S., Bahal, R., Wheeler, S. E., Procopio, E. M., Kim, J., Joyce, S. C., Contrucci, S., Wang, Y., Chiosea, S. I., Lathrop, K. L., Watkins, S., Grandis, J. R., Armitage, B. A., and Ly, D. H. (2013) Antitumor Effects of EGFR Antisense Guanidine-Based Peptide Nucleic Acids in Cancer Models. *ACS Chem. Biol.* 8, 345–352.
- (57) Bertrand, H., Granzhan, A., Monchaud, D., Saettel, N., Guillot, R., Clifford, S., Guedin, A., Mergny, J.-L., and Teulade-Fichou, M.-P. (2011) Recognition of G-Quadruplex DNA by Triangular Star-Shaped Compounds: With or Without Side Chains? *Chem.—Eur. J.* 17, 4529–4539.
- (58) Sparapani, S., Haider, S. M., Doria, F., Gunaratnam, M., and Neidle, S. (2010) Rational Design of Acridine-Based Ligands with Selectivity for Human Telomeric Quadruplexes. *J. Am. Chem. Soc.* 132, 12263–12272.
- (59) Campbell, N. H., Parkinson, G. N., Reszka, A. P., and Neidle, S. (2008) Structural Basis of DNA Quadruplex Recognition by an Acridine Drug. *J. Am. Chem. Soc.* 130, 6722–6724.
- (60) Maga, G., Villani, G., Tillement, V., Stucki, M., Locatelli, G. A., Frouin, I., Spadari, S., and Hübscher, U. (2001) Okazaki fragment processing: Modulation of the strand displacement activity of DNA polymerase  $\delta$  by the concerted action of replication protein A, proliferating cell nuclear antigen, and flap endonuclease-1. *Proc. Natl. Acad. Sci. U.S.A.* 98, 14298–14303.
- (61) Ho, T. V., Guainazzi, A., Derkunt, S. B., Enou, M., and Scharer, O. D. (2011) Structure-dependent bypass of DNA interstrand crosslinks by translesion synthesis polymerases. *Nucleic Acids Res.* 39, 7455–7464.
- (62) Murat, P., Zhong, J., Lekieffre, L., Cowieson, N. P., Clancy, J. L., Preiss, T., Balasubramanian, S., Khanna, R., and Tellam, J. (2014) G-quadruplexes regulate Epstein-Barr virus-encoded nuclear antigen 1 mRNA translation. *Nat. Chem. Biol.* 10, 358–364.
- (63) Dragulescu-Andrasi, A., Rapireddy, S., Frezza, B. M., Gayathri, C., Gil, R. R., and Ly, D. H. (2006) A Simple  $\gamma$ -Backbone Modification Preorganizes Peptide Nucleic Acid into a Helical Structure. *J. Am. Chem. Soc.* 128, 10258–10267.
- (64) Zhou, P., Dragulescu-Andrasi, A., Bhattacharya, B., O'Keefe, H., Vatta, P., Hyldig-Nielsen, J. J., and Ly, D. H. (2006) Synthesis of cell-permeable peptide nucleic acids and characterization of their hybridization and uptake properties. *Bioorg. Med. Chem. Lett.* 16, 4931–4935.